A simple method of extrapolating the coexistence curve and predicting the melting point depression curve from cloud point data for polymer–diluent systems

Kenneth S. McGuire, Anand Laxminarayan and Douglas R. Lloyd*
Department of Chemical Engineering, Centre for Polymer Research, The University of Texas at Austin, Austin, TX 78712, USA
(Received 29 September 1993; revised 19 January 1994)

This paper presents a quick, useful method for obtaining an equilibrium phase diagram (including the melting point depression curve) for a semicrystalline polymer–diluent mixture from cloud point data. Good agreement was obtained between the theoretically predicted and experimentally generated equilibrium crystallization curves in spite of simplifying assumptions. An accurate extrapolation of the coexistence curve to regions in the phase diagram where experimental generation of cloud point data is not possible was also obtained. Flory's original polymer swelling theory was used to determine the complete phase diagram. In the system studied (isotactic polypropylene in diphenyl ether), the interaction parameter was assumed to be a function of temperature only. Cloud points were generated experimentally, and an interaction parameter was determined at each temperature. A melting point depression curve was calculated from the temperature dependent interaction parameter and compared with experimentally determined equilibrium melting points. The resulting phase diagram was used to interpret the morphology of microporous structures prepared by the thermally induced phase separation mechanism.

(Keywords: interaction parameter; phase separation; semicrystalline polymer)

INTRODUCTION

Phase diagrams provide crucial information about the phase behaviour of polymer–diluent systems. When thermal energy is removed from a homogeneous polymer–diluent mixture, thermally induced phase separation (TIPS) can occur. The TIPS process has many applications in polymer science, including the formation of microporous membranes[1–7] and foams[8]. If the polymer is semicrystalline, then phase separation can occur via solid–liquid, liquid–liquid, or liquid–solid phase separation depending on the polymer–diluent interactions, the composition of the mixture and the thermal driving force[9]. Because the phase separation mechanism significantly influences the morphology of the resulting microporous structure[1], a phase diagram is essential for predicting the resulting morphology. Kim and coworkers have done thorough studies on the thermodynamics of polymer–diluent systems[3,10–12] with emphasis given to the generation of equilibrium phase diagrams. Kim used an equation of state theory to predict the phase behaviour, and although the results show good agreement with experiments, the generation of the required thermodynamic data is extremely time consuming. Cloud point measurements are quick and easy to make. Using Flory's simple lattice model, the following method was devised to generate the entire phase diagram (including the melting point depression curve) from only a few cloud point measurements.

THEORY

Flory has derived expressions relating the free energy of a polymer–diluent system to the volume fractions of the species present[13]. Phase separation results in the formation of two coexisting phases of differing polymer compositions. Equating polymer chemical potentials in the two phases gives two equations describing the binodal or coexistence curve

$$[(\phi_2^\beta)^2-(\phi_2^\alpha)^2]\chi_1=\ln\left(\frac{1-\phi_2^\alpha}{1-\phi_2^\beta}\right)+\left(1-\frac{1}{x}\right)(\phi_2^\alpha-\phi_2^\beta) \quad (1)$$

and

$$x[(1-\phi_2^\beta)^2-(1-\phi_2^\alpha)^2]\chi_1=\ln\left(\frac{\phi_2^\alpha}{\phi_2^\beta}\right)+(x-1)(\phi_2^\alpha-\phi_2^\beta) \quad (2)$$

where χ_1 is the interaction parameter based on the diluent molar volume, ϕ_2^α is the volume fraction of the polymer in phase α, ϕ_2^β is the volume fraction of the polymer in phase β and x is the ratio of the polymer molar volume to the diluent molar volume.

Similarly, crystallization of the polymer yields a crystal phase of pure polymer and a melt phase of polymer composition ϕ_2. By equating the chemical potentials of the polymer in the melt and crystal phases, the melting point depression curve can be calculated. If the interaction parameter is assumed to have a temperature dependence of $\chi_1(T)=\alpha+\beta/T$, as is often the case with polymer solutions, then the melting point equation can

---

*To whom correspondence should be addressed

0032-3861/94/20/4404-04

be written as[14]

$$\frac{1}{T_m} = \left[1+\frac{R\beta}{\Delta H_u}(1-\phi_2)^2\right]^{-1}\left\{\frac{1}{T_m^\circ}+\frac{R}{\Delta H_u}\times\left[\left(1-\frac{1}{x}\right)(1-\phi_2)-\frac{\ln\phi_2}{x}-\alpha(1-\phi_2)^2\right]\right\} \quad (3)$$

where T_m is the melting point of the diluted polymer, T_m° is the melting point of the pure polymer, R is the gas constant and ΔH_u is the heat of fusion per mole of repeat units.

EXPERIMENTAL

Isotactic polypropylene (iPP) of $M_w = 168\,000$ was obtained from Fina and diphenyl ether (DPE; 99% purity) was obtained from Aldrich. All chemicals were used without further purification.

Polymer–diluent sample preparation is fully described elsewhere[3]. Cloud points were determined as follows (a more detailed description is given elsewhere[2]). Small slivers (ca. 2 × 2 × 1 mm) of the solid polymer–diluent sample were cut with a razor blade, sandwiched between two glass cover slips and sealed with vacuum grease to prevent diluent loss by evaporation. The sealed sample was placed on a Linkam HFS-91 hot stage. The hot stage was placed on the platform of an optical microscope. The temperature of the stage was controlled by a Linkam TMS-91 controller. The sample was heated to 433 K for 5–10 min to assure homogeneity and to remove any prior thermal history. Light of wavelength 628 nm was passed through the sample, and the intensity of the transmitted light was monitored as the sample was cooled at a controlled rate. The onset of the change in intensity was taken as the cloud point.

Equilibrium melting points were measured following the method of Hoffman and Weeks[15]. Samples of approximately 5 mg were placed in sample pans and then into a Perkin–Elmer DSC-7. The samples were heated to 473 K, cooled to the desired crystallization temperature at the maximum attainable cooling rate (ca. 100 K min^{-1}), allowed to crystallize for 1 h at various degrees of supercooling of greater than 40 K and then melted at a rate of 10 K min^{-1}.

Scanning electron micrographs of membranes made by TIPS were obtained as follows. A sample similar to those used for cloud point measurements was removed from the hot stage following the appropriate thermal treatment. The sample was immersed in liquid nitrogen to freeze the structure. The diphenyl ether was extracted with methanol (Sigma, spectrophotometric grade) and the resulting microporous structure was dried under vacuum. Finally, the sample was fractured in liquid nitrogen and coated with 5–12 nm of gold–palladium using a sputtering coater (Commonwealth Model 3, Pelco). The cross-section was photographed on a JOEL JSN-35C microscope under an accelerating voltage of 25 kV.

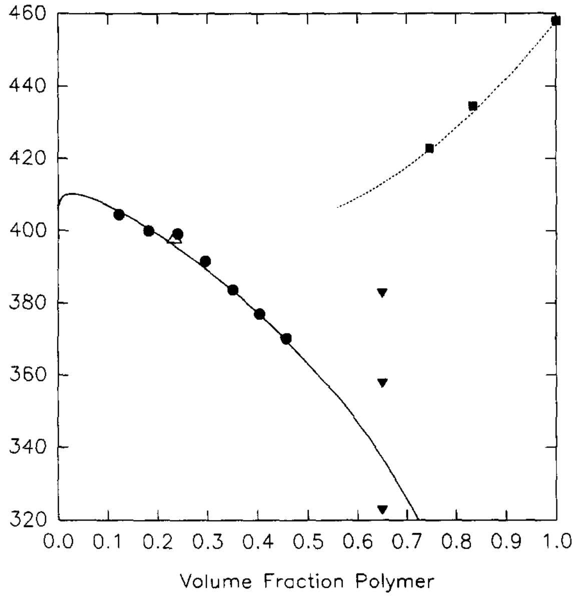

Figure 1 Phase diagram for iPP–DPE: (●) cloud points; (■) experimental equilibrium melting points; (△) true coexistence point; (▼) phase separation conditions for *Figures 3–5*; (——) theoretical coexistence curve; (····) theoretical melting point depression curve with $T_m^\circ = 458$ K and $\Delta H_u = 2400$ cal mol^{-1} repeat units

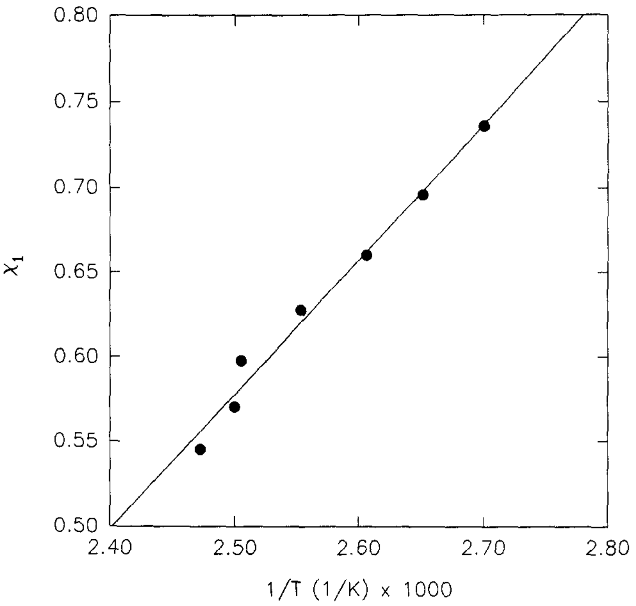

Figure 2 Temperature dependence of the interaction parameter for iPP–DPE

RESULTS AND DISCUSSION

Cloud points were determined for seven volume fractions of polymer ranging from 0.12 to 0.46, as shown in *Figure 1*. The cloud points were independent of cooling rate within the range 10–50 K min^{-1}. As a first approximation, the cloud points were assumed to be representative of the coexistence curve. The value of x used in equations (1), (2) and (3) was taken from M_w. The molecular weight of the sample used in this study is high enough such that terms containing $1/x$ are negligible. By simultaneously solving equations (1) and (2) with ϕ_2^β (the cloud point) known, and by assuming that χ_1 is not concentration dependent, χ_1 was determined as a function of temperature. *Figure 2* shows that a plot of χ_1 against $1/T$ gives a straight line. Using this temperature dependent interaction parameter, the coexistence curve was plotted in *Figure 1* along with the cloud points. The generation of the coexistence curve in this manner is essentially an elegant curve fit based on Flory's theory.

To generate the expected melting point depression curve, the plot of χ_1 against $1/T$ was extrapolated to the equilibrium melting point of the pure polymer, which was taken as 458 K[16]. Then, the melting point depression curve (dotted line in *Figure 1*) was generated using equation (3) and a heat of fusion for iPP of 2400 cal mol^{-1} repeat units[17] (1 cal = 4.2 J).

Figure 1 is tentatively assumed to be the equilibrium phase diagram and was generated from cloud point data alone. The assumptions made in generating this phase diagram are evaluated below.

To calculate the interaction parameter at each temperature, it was assumed that the cloud point curve was representative of the coexistence curve. For a polydisperse system, however, this is not the case[18–20]. Fina specifies a polydispersity of 6.0 for the iPP used in this study. A true coexistence point was generated by an extraction method. A 0.12 polymer volume fraction iPP–DPE sample (2 g) was prepared in a test tube. The test tube was then purged with nitrogen and heat sealed. The sealed test tube was heated to 433 K in a convection oven for two days to form a homogeneous mixture. Next, the sealed sample was quenched in a silicone oil bath at 398 K and was left overnight until two distinct macroscopic phases were observed. The tube was then removed from the oil bath and quenched into liquid nitrogen. The composition of the polymer-rich phase was determined by diluent extraction. This composition was taken to be the true coexistence point and is shown in *Figure 1* along with the cloud points. The amount of polymer present in the diluent-rich phase was too small to be detected by the extraction method. The extraction method for determining true coexistence compositions is time consuming owing to the long time required for diluent extraction and evaporation. A quicker method is outlined below.

A 2 g sample was prepared as above, immersed in the silicone oil bath overnight and quenched into liquid nitrogen upon observation of two macroscopic phases as before. To determine the composition of the polymer-rich phase, the cloud point of a sample of this phase was measured. The cloud points of samples of known compositions were determined above (the circular symbols in *Figure 1*), so comparison of the cloud point of an unknown composition with this curve yields the composition of the polymer-rich phase. For example, the cloud point of the polymer-rich phase generated by phase separating a sample of 0.12 polymer volume fraction at 398 K was found to be 398.4 ± 0.4 K. From *Figure 1*, the cloud point composition at 398.4 K is roughly a 0.25 polymer volume fraction. Two quench temperatures were tested in this manner (393 and 398 K) and the quench temperatures and cloud point temperatures agreed to within 0.5 K in both cases.

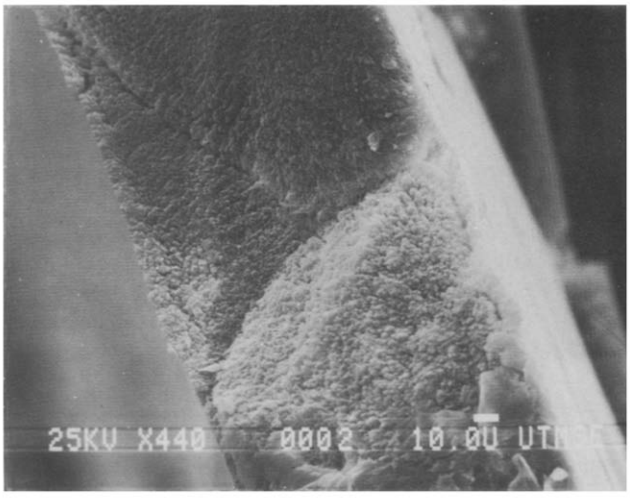

Figure 3 Micrograph of the cross-section of a 0.65 iPP volume fraction sample quenched to 383 K

Based on the extraction study and the supplementary quench/cloud point experiments, it is concluded that for the system studied here, within the accuracy of the experimental studies, the cloud point curve is representative of the coexistence curve.

In generating the phase diagram, it was also assumed that the temperature dependence of the interaction parameter could be extrapolated to higher temperatures to generate a melting point depression curve. To check the accuracy of the melting point depression curve, equilibrium melting points were determined[15]. As shown in *Figure 1*, the experimental equilibrium melting point of the pure polymer coincides with that reported by Clark and Hoffman[16] and lies on the predicted melting point depression curve. The value for the heat of fusion, 2400 cal mol^{-1} repeat units, was used to generate the theoretical curve[17]. The melting points for 0.75 and 0.83 polymer volume fractions fall on the predicted curve, confirming the extrapolation of the temperature dependence of χ_1. Melting points of samples with polymer volume fractions less than 0.75 could not be measured owing to interference from liquid–liquid phase separation.

It should be noted that the portion of the binodal that passes beneath the melting point depression curve represents only a kinetically attainable state, and as such is not actually a part of the equilibrium phase diagram. However, because the cloud points were measured at a cooling rate of 10 K min^{-1}, liquid–liquid phase separation was initiated before the polymer crystallized from solution up to $\phi_2 = 0.45$.

One benefit of generating a phase diagram from cloud points (which may be measured below the equilibrium melting point of the polymer, as described in the last paragraph) is that it allows for an accurate extrapolation of the coexistence curve to regions well below the melting point depression curve where experimental cloud points are unattainable. This allows for prediction of the phase separation mechanism (and hence the resulting morphology) for quenches well below the equilibrium melting point of the polymer mixture. Consider an iPP–DPE mixture of 0.65 iPP volume fraction quenched to 383 K (*Figure 3*). At this temperature, polymer crystallizes from solution without interference from liquid–liquid phase separation. The resulting morphology is relatively dense spherulites, as predicted by the phase diagram.

Next, consider a 0.65 iPP volume fraction sample quenched to 323 K (*Figure 4*). At this temperature, liquid–liquid phase separation should occur with subsequent polymer crystallization. Upon extracting the DPE, a cellular structure results, which is characteristic of a polymer mixture undergoing liquid–liquid TIPS. The size of the resulting cells is dependent on the growth rate of the cellular domains and the crystallization rate of the polymer[21].

Finally, consider a 0.65 iPP volume fraction sample quenched to 358 K (*Figure 5*). Here, the sample is at a temperature lower than the equilibrium melting point of the polymer, and polymer is expected to crystallize from solution in the form of spherulites (as was the case in *Figure 3*). Initially, polymer begins to crystallize in

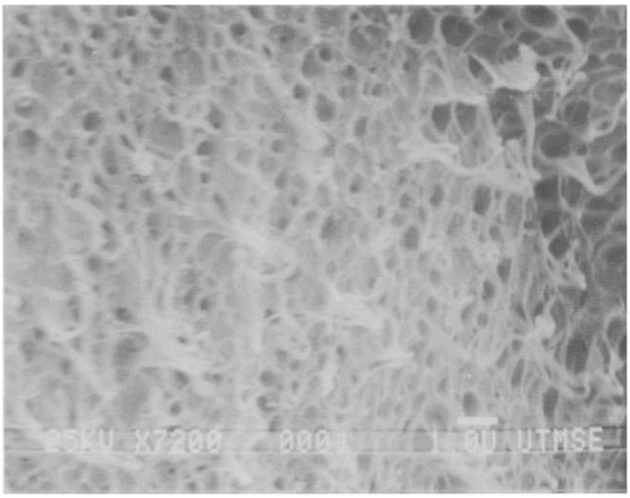

Figure 4 Micrograph of the cross-section of a 0.65 iPP volume fraction sample quenched to 323 K

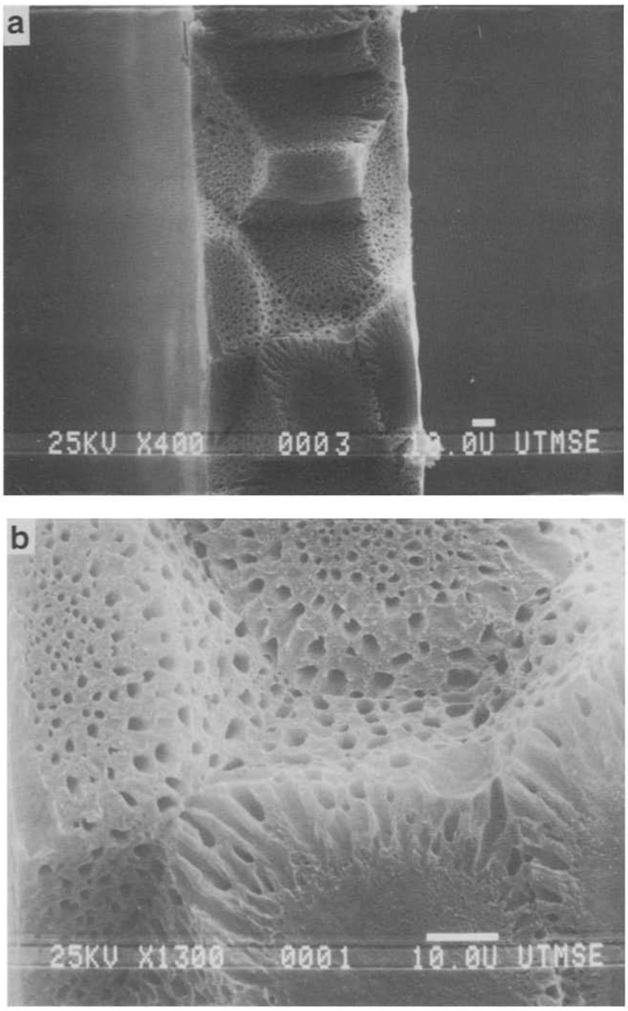

Figure 5 Micrographs of the cross-section of a 0.65 iPP volume fraction sample quenched to 358 K: (a) low magnification; (b) high magnification

spherulites. However, as crystallization proceeds, diluent is rejected to the spherulite growth front, and the polymer concentration at the front decreases. Eventually, the concentration of the front reaches the limit of miscibility, and liquid–liquid phase separation occurs at the growth front. This phenomenon has been observed in polymer blends[22–25] and was observed in this study as the phase separation occurred using an optical microscope. The resulting morphology is that of spherulites with dense cores and a cellular structure near the fringes of the impinged spherulites.

CONCLUSIONS

Cloud point data for a semicrystalline polymer–diluent system can be used to generate an entire phase diagram using Flory's original lattice theory to describe the polymer–diluent thermodynamics. For the polydisperse iPP–DPE system, these predictions agree with experimental coexistence points and experimental melting points. Further, it was determined for the system under study that the cloud point curve is representative of the coexistence curve. Finally, morphologies of systems resulting from deep quenches into or near the kinetically attainable miscibility gap can be explained by extending the coexistence curve to temperatures beyond the range of kinetically attainable cloud points.

ACKNOWLEDGEMENTS

The authors gratefully acknowledge the continued generous financial support of the Central Research Technology Development Laboratory of the 3M Company (St Paul, MN), the Texas Advanced Technology Program and the Department of Defense.

REFERENCES

1 Lloyd, D. R., Kinzer, K. E. and Tseng, H. S. *J. Membr. Sci.* 1990, **52**, 239
2 Lloyd, D. R., Kim, S. S. and Kinzer, K. E. *J. Membr. Sci.* 1991, **64**, 1
3 Kim, S. S. and Lloyd, D. R. *J. Membr. Sci.* 1991, **64**, 13
4 Kim, S. S., Lim, G. B. A., Alwattari, A. A., Wang, Y. F. and Lloyd, D. R. *J. Membr. Sci.* 1991, **64**, 41
5 Alwattari, A. A. and Lloyd, D. R. *J. Membr. Sci.* 1991, **64**, 55
6 Lim, G. B. A., Kim, S. S., Ye, Q., Wang, Y. F. and Lloyd, D. R. *J. Membr. Sci.* 1991, **64**, 31
7 McGuire, K. S., Lloyd, D. R. and Lim, G. B. A. *J. Membr. Sci.* 1993, **79**, 27
8 Williams, J. M. and Moore, J. E. *Polymer* 1987, **28**, 1950
9 Kim, S. S. 'Thermodynamics and Structural Study of TIPS Membranes', Dissertation, The University of Texas at Austin, 1990, Chs 2 and 3
10 Kim, S. S. and Lloyd, D. R. *Polymer* 1992, **33**, 1026
11 Kim, S. S. and Lloyd, D. R. *Polymer* 1992, **33**, 1036
12 Kim, S. S. and Lloyd, D. R. *Polymer* 1992, **33**, 1047
13 Flory, P. J. 'Principles of Polymer Chemistry', Cornell University Press, Ithaca, NY, 1953, Chs XII and XIII
14 Burghardt, W. R. *Macromolecules* 1989, **22**, 2482
15 Hoffman, J. D. and Weeks, J. J. *J. Res. Nat. Bur. Stand., Sect. A* 1962, **66**, 13
16 Clark, E. J. and Hoffman, J. D. *Macromolecules* 1984, **17**, 878
17 Kirshenbaum, I., Wilchinsky, Z. W. and Groten, B. *J. Appl. Polym. Sci.* 1964, **8**, 2723
18 Koningsveld, R. and Staverman, A. J. *J. Polym. Sci.* (*A-2*) 1968, **6**, 305
19 Koningsveld, R. and Staverman, A. J. *J. Polym. Sci.* (*A-2*) 1968, **6**, 325
20 Koningsveld, R. and Staverman, A. J. *J. Polym. Sci.* (*A-2*) 1968, **6**, 349
21 Laxminarayan, A., McGuire, K. S., Kim, S. S. and Lloyd, D. R. *Polymer* in press
22 Tanaka, H. and Nishi, T. *Phys. Rev. Lett.* 1985, **55**, 1102
23 Tanaka, H. and Nishi, T. *Phys. Rev. A* 1989, **39**, 783
24 Li, Y., Stein, M. and Jungnickel, B.-J. *Colloid Polym. Sci.* 1991, **269**, 772
25 Shibanov, Y. D. and Godovsky, Y. K. *Makromol. Chem.* 1991, **44**, 61